


## ORIGINAL RESEARCH

# Application of metaheuristic algorithms in prediction of earthquake peak ground acceleration

Surya Prakash Challagulla<sup>1</sup> | Ashok Kumar Suluguru<sup>2</sup> | Ehsan Noroozinejad Farsangi<sup>3</sup>  | Mounika Manne<sup>4</sup>

<sup>1</sup>Department of Civil Engineering, Koneru Lakshmaiah Education Foundation, Vaddeswaram, Andhra Pradesh, India

<sup>2</sup>Department of Civil Engineering, Malla Reddy Engineering College, Maisammaguda, Telangana, India

<sup>3</sup>Faculty of Civil and Surveying Engineering, Graduate University of Advanced Technology, Kerman, Iran

<sup>4</sup>Department of Civil Engineering, Birla Institute of Technology and Science -Pilani, Hyderabad, Telangana, India

**Correspondence**

Ehsan Noroozinejad Farsangi, Faculty of Civil and Surveying Engineering, Graduate University of Advanced Technology, Kerman, Iran.  
Email: noroozinejad@kgut.ac.ir

**Abstract**

The seismic resilience of a structure has been evaluated using peak ground acceleration (PGA). Ground motion parameters such as source characteristics, local site conditions are used to forecast the PGA of the ground motion. This paper aims to develop an Artificial Neural Network (ANN) based model to predict the PGA. Here, hypocentral distance ( $R_{hypo}$ ), shear wave velocity ( $V_{s30}$ ), and moment magnitude ( $M_w$ ), are used as input parameters. The model uses 12,706 ground motion recordings from 283 earthquakes from the revised NGA-West2 database supplied by Pacific Engineering Research Centre. Among the whole data, 70% of the data is set for training, 15% for validation, and 15% for testing the network. The  $R$  value derived from the testing dataset is 0.952, indicating the excellent performance of a network. An extensive parametric study is conducted with the PGA values, and the results indicate that the PGA increases with the magnitude and decreases with the hypocentral distance. The predicted PGA values from the present study are comparable with those from the existing relationships in the global database. The generated ANN model is further verified by comparing the predicted and recorded PGA values of an actual recorded event.

## 1 | INTRODUCTION

An important research topic for seismic hazard analysis is the prediction of ground motion intensity measures (IMs) in terms of distance, magnitude, and other factors utilizing attenuation relationships [1]. For a particular site classification, the most typically mapped ground motion IMs are peak ground velocity (PGV), peak ground acceleration (PGA), and spectral acceleration (SA). These calculations are known as attenuation relationships, and they express ground motion as a function of distance and magnitude, as well as other variables like faulting type [2]. In the past, such relationships have been developed for numerous locations of the world [3, 4, 13–18, 5–12]. Most of these studies use regression analysis. Regression analysis is not effective in extracting the nonlinear behaviour in the ground motion database [19]. This issue can be solved by using machine learning techniques to establish a ground motion prediction equation. Machine learning techniques can capture the non-linear behaviour present in the data.

Few studies have used Artificial Neural Networks to predict the ground motion value. The peak ground acceleration of the Taiwan region was estimated by using the back-propagation neural network model [20]. Peak ground motion parameters like PGA, PGV were evaluated for Europe region by utilizing the Artificial Neural Networks with the limited ground motion data [21]. Neural Networks were used to predict the earthquakes with higher magnitudes in Tokyo [22]. Feed-Forward Back Propagation algorithm was utilized to determine the PGA in north western Turkey [23]. Deep Neural Networks were utilized to generate the Ground Motion Model (GMM) for the Legnica-Głogów Copper District in Poland [24]. Artificial neural networks were used to establish an attenuation relationship for PGA estimate utilizing Indian strong-motion data [25]. Very recently, a region-specific Neural-Network based ground motion prediction equation was generated [26]. Empirical ground motion models were developed for Southern California region for small magnitude earthquakes using feed-forward neural networks [27]. These studies suggested that Neural

This is an open access article under the terms of the [Creative Commons Attribution](https://creativecommons.org/licenses/by/4.0/) License, which permits use, distribution and reproduction in any medium, provided the original work is properly cited.

© 2023 The Authors. *The Journal of Engineering* published by John Wiley & Sons Ltd on behalf of The Institution of Engineering and Technology.

Network approach to ground motion prediction equation could be an efficient tool. And, from the above studies, it can be inferred that all the ground motion prediction equations were region specific and developed using limited ground motion data. Hence, there is a scope to develop a generalized ground motion prediction equation by considering the vast global database.

In this regard, this study utilizes the Artificial Neural Networks for ground motion prediction using the global database. ANN is a strong tool for addressing complex issues, and it is particularly effective for civil engineering challenges [28–32]. Here, the prediction equation was built utilizing 12,706 data points obtained from 283 earthquakes from the revised NGA-West2 database using neural networks.  $M_w$ ,  $R_{hypo}$ , and  $V_{s30}$  are selected as the inputs for this study. The output variable considered is Peak Ground Acceleration (PGA). Sensitivity analysis is conducted to determine the essential inputs and their relative relevance on the model output (PGA). Finally, the developed ANN based ground motion prediction model is compared with the existing prediction equations. Further, the model is validated by comparing the predicted ground motion values with the actual recorded data. The advantages of modelling of ANN over that of statistical linear and non-linear regression are: (i) the functional design expression or its form need not be assumed a priori as in the case of non-linear regression, (ii) the degree of non-linearity of independent parameters also need not be assumed a priori, (iii) flexibility of varying the network architecture easily for accurate modelling and prediction which is independent of functional approximation, and (iv) the ease of coming up with generalized design expression for the chosen, most accurate simulation and prediction.

The following is the structure of the paper: Section 2 shows the research methodology. Section 3 describes the earthquake data. The specifics of the Artificial Neural Network and the outcomes of the ANN model are presented in Section 4. The procedure for generating the prediction equation using ANN is presented in Section 5. Sections 6 and 7 show the parametric and sensitivity analysis, respectively. Section 8 offers the validation of predictive relation. In the final section, simple conclusions are made (i.e., Section 9).

## 2 | RESEARCH METHODOLOGY

The relevance of the research is that it employs the machine learning (ML) technique known as Artificial Neural Networks (ANNs) for the prediction and comparison of PGA of ground motions with the conventional approach. The prediction model was created using the optimized AI architecture and functionalities. The NGA-West2 database was used to get the strong-motion data. The input parameters include hypocentral distance ( $R_{hypo}$ ), shear wave velocity ( $V_{s30}$ ), and moment magnitude ( $M_w$ ). The output variable is the Peak Ground Acceleration. The dataset is separated into three parts: training, validation, and testing. The prediction equation is created by selecting the best ANN model architecture and dataset.

The parametric research is carried out using predicted PGA values for various  $R_{hypo}$ ,  $V_{s30}$ , and  $M_w$  combinations. A sensitivity analysis was performed to identify the critical parameters and their relative importance on predicted model outputs. Finally, the constructed prediction equation is verified by comparing predicted output values to those obtained from earlier developed equations. Figure 1 depicts the investigation's methodology.

## 3 | EARTHQUAKE DATA

Data for this study was collected from the updated PEER-NGA-West2 database available in <https://peer.berkeley.edu/research/nga-west-2>. The earthquake data consists of 12,706 ground motion recordings from 283 earthquake events across the globe. The hypocentral distance ( $R_{hypo}$ ), average shear wave velocity ( $V_{s30}$ ) over the top 30 m of soil, and moment magnitude ( $M_w$ ) are considered as inputs for generating the model. Moment magnitude represents the source characteristics of earthquake. Hypocentral distance represents the distance from the source to the site. Because this measure is based on the earthquake's epicentre and focal depth, it can offer a more precise depiction of the source-to-site distance [19, 33, 34].

Figure 2 shows the magnitude variation as a function of hypocentral distance, illustrating the various magnitudes and the distribution of hypocentral distance of events. The variation between PGA and hypocentral distance is shown in Figure 3. The earthquake data used in the current study includes data from both rock sites and soil sites.

## 4 | ARTIFICIAL NEURAL NETWORKS

To forecast the Peak Ground Acceleration (PGA), a Neural Network based prediction relationship has been generated. Previous research has shown that such relationships can be useful, and numerous studies have found identical ANN-based prediction correlations concerning various problems [35–38]. In the MATLAB R2019b environment, a feed-forward neural network was built. Transfer functions, also known as activation functions and output functions, are the functions that control the input-output behaviour. Linear and Tan-sigmoid transfer functions were chosen between hidden-output nodes and input-hidden nodes, respectively. The Levenberg–Marquardt (LM) method was used to train the network. Kenneth Levenberg and Donald Marquardt created the Levenberg–Marquardt method to offer numerical solutions to non-linear function issues. This neural network training approach is quick and offers consistent convergence [39]. In proportions of 70%, 15%, and 15%, the data is randomly divided into training, validation, and testing. For this phase, the present ANN model finds this percentage to be optimum. The variables should be normalised between  $-1.0$  and  $1.0$  before being fed into the ANN model. In general, normalisation is done to guarantee that all variables are given the same amount of importance [40]. The following formula is used to calculate the normalised value of  $x$ , with  $x_{\min}$  and  $x_{\max}$ , being

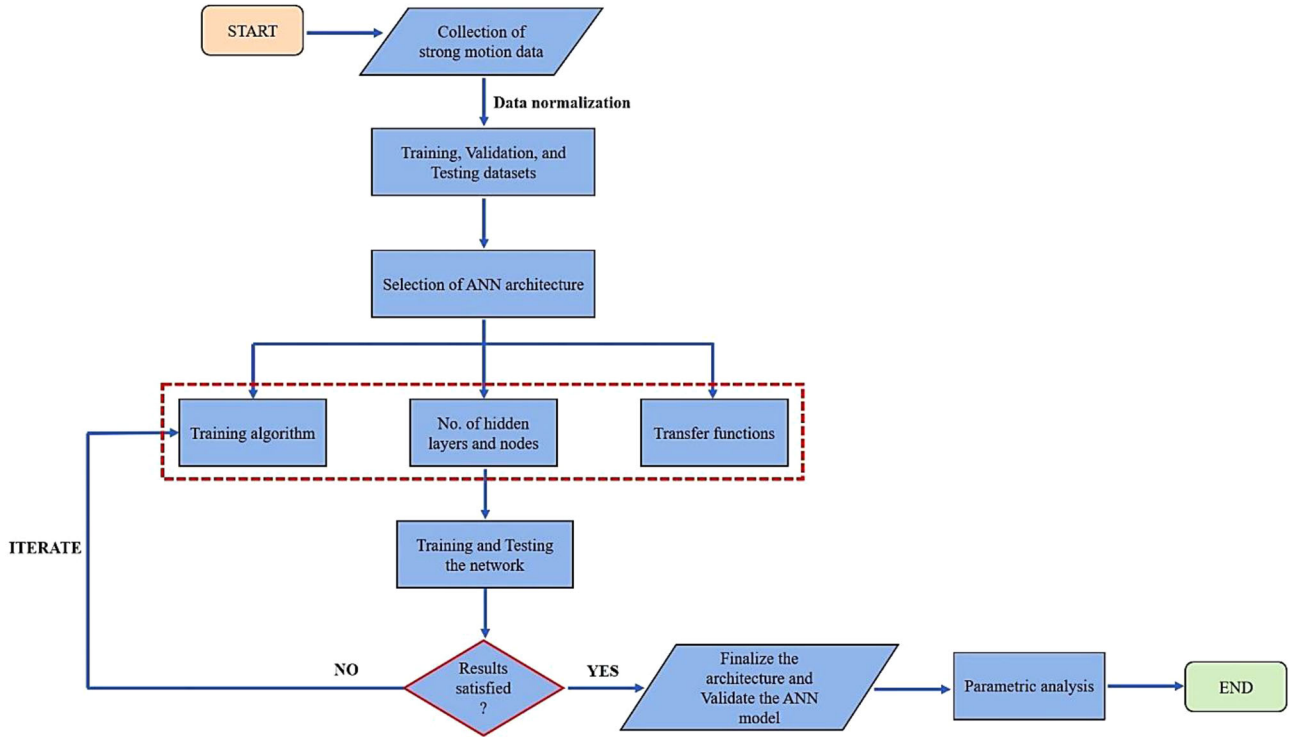


FIGURE 1 A framework showing research methodology.

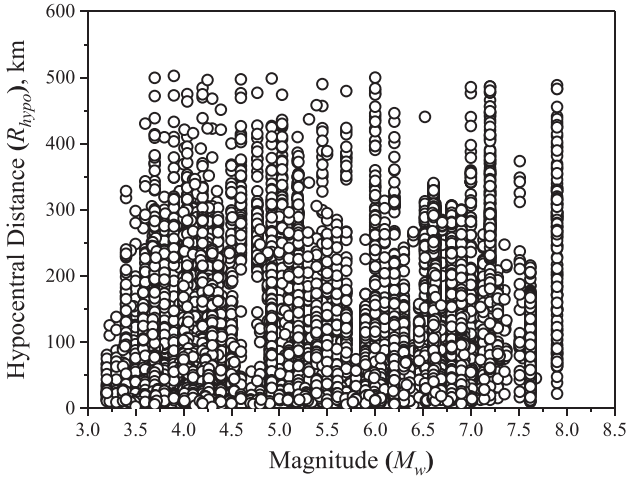


FIGURE 2 Variation of magnitude with hypocentral distance.

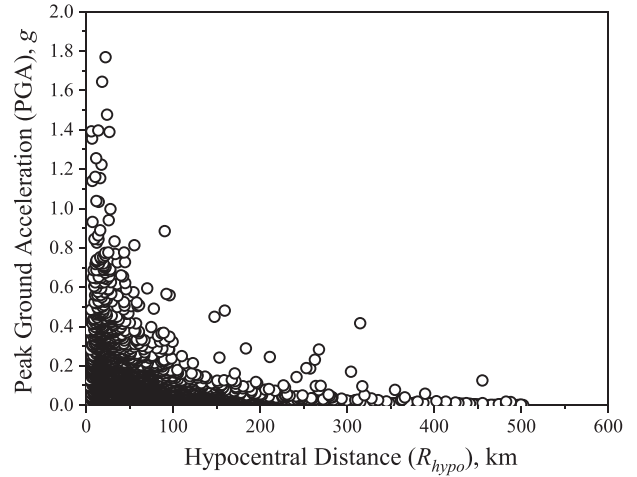


FIGURE 3 Variation of peak ground acceleration (PGA) with hypocentral distance.

the minimum and maximum values, respectively:

$$\text{Normalized value, } \mathbf{x}_n = \frac{2(\mathbf{x} - \mathbf{x}_{\min})}{(\mathbf{x}_{\max} - \mathbf{x}_{\min})} - 1 \quad (1)$$

To ensure that the ANN model performs optimally, an optimal number of hidden nodes must be used. The ideal number of hidden nodes is regarded to be between 1 and  $(2j+1)$ , where  $j$  is the number of inputs that generates the lowest mean squared error (MSE) [41]. Alternatively, a trial-and-error method can be used to determine the number of hidden nodes which is

a tedious task. The average difference between values predicted by a regression model and the actual value observed is measured by the term “mean square error.” It is determined by taking the average of all squared differences over the full dataset. Since it better reflects how well our predictions correlate with reality, MSE is useful for regression situations. Hence, MSE is chosen as a parameter to select optimum number of hidden nodes. Here, the input parameters are four (magnitude, hypocentral distance,  $\log_{10}$ -scaled hypocentral distance, and  $\log_{10}$ -scaled shear wave velocity). ANN models were

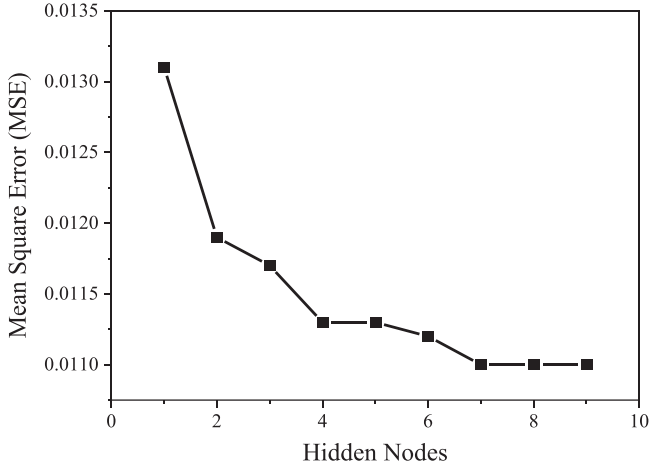


FIGURE 4 Mean squared error (MSE) versus hidden nodes.

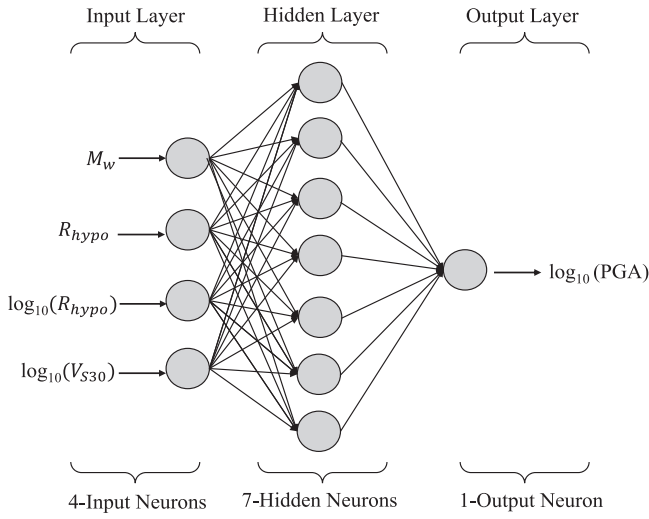


FIGURE 5 Architecture of the developed artificial neural network (ANN) model.

generated with hidden nodes varying from 1 to 9. The model with the lowest error was selected, and the nodes matching to that number was deemed optimal as shown in Figure 4, which is seven in this case. Thus, by selecting four hidden nodes, the highest performing and optimal ANN model was found, and the ANN model was named ANN 4-7-1 in this study. Figure 5 depicts the model's architecture to aid comprehension. As seen in Figure 5, the log-scaled ground motion parameter ( $\log_{10}(\text{PGA})$ ) is predicted using the magnitude ( $M_w$ ), hypocentral distance ( $R_{hypo}$ ),  $\log_{10}$ -scaled shear wave velocity ( $\log_{10}(V_{s30})$ ), and  $\log_{10}$ -scaled hypocentral distance ( $\log_{10}(R_{hypo})$ ). This functional form was selected to approximate the often-found correlations between ground motion parameters and predictor variables [42].

The performance assessment functions used in this study to test the ANN models' predictive accuracy are Mean Absolute Error (MAE), Coefficient of Correlation ( $R$ ), and Mean Squared Error (MSE). The model's performance is summarised in Table 1. The functions for measuring performance are listed

TABLE 1 Performance of ANN-4-7-1

Data	MSE	MAE	R
Training	0.0057	0.0421	0.948
Testing	0.0046	0.0422	0.952

below:

$$R = \sqrt{\frac{\sum Y_m^2 - \frac{(\sum (Y_m - Y_p))^2}{N}}{\sum Y_m^2}} \quad (2)$$

$$MSE = \frac{\sum (Y_m - Y_p)^2}{N} \quad (3)$$

$$MAE = \frac{\sum |Y_m - Y_p|}{N} \quad (4)$$

where  $Y_m$  and  $Y_p$  are the actual and predicted values.

The  $R$ -value is used to assess the fit between predicted and actual values as well as their relative correlation. As a result, it must therefore be as high as possible. MAE and MSE should be kept to a minimum [43]. The complete correlation between the actual and anticipated PGA is shown in Figure 6. As a result, the model explicitly has significant predictive capacity within the data range used to generate it.

## 5 | PREDICTIVE EXPRESSIONS USING ANN

In this work, the model equation for  $\log_{10}(\text{PGA})$  was derived using the ANN-4-7-1 model. The following equation is used to produce a predictive relationship utilising the weights of an ANN model by linking the input and output parameters [44]:

$$Y_n = f_o \left\{ b_o + \sum_{k=1}^b \left[ w_k * f_b \left( b_{bk} + \sum_{i=1}^m w_{ik} X_{ni} \right) \right] \right\} \quad (5)$$

where  $w_k$  = weight connection between hidden layer neuron ( $k$ ) and single output neuron;  $b_{bk}$  =  $k^{\text{th}}$  hidden neuron bias;  $w_{ik}$  = weight between the input and hidden layer neuron ( $k$ );  $b_o$  = bias of the output layer;  $X_{ni}$  = input parameter;  $f_o$  = transfer function of the output layer (Linear function); and  $f_b$  = transfer function of the hidden layer (Tan-sigmoid).

The biases and weights listed in Table 2 were inserted into Equation (5) to generate the  $\log_{10}(\text{PGA})$  prediction equation. The bias weights as shown in Table 2 make the ANN model more general and robust. Using the input variables, the formulas in Equations (6)–(15) are used to get the normalised value of log-scaled ground motion parameter ( $\log_{10}(\text{PGA})$ ).

$$a = -1.5974 \times M_w - 0.9285 \times R_{hypo} + 0.2424 \times \log_{10}(R_{hypo}) - 1.3628 \times \log_{10}(V_{s30}) + 1.7077 \quad (6)$$

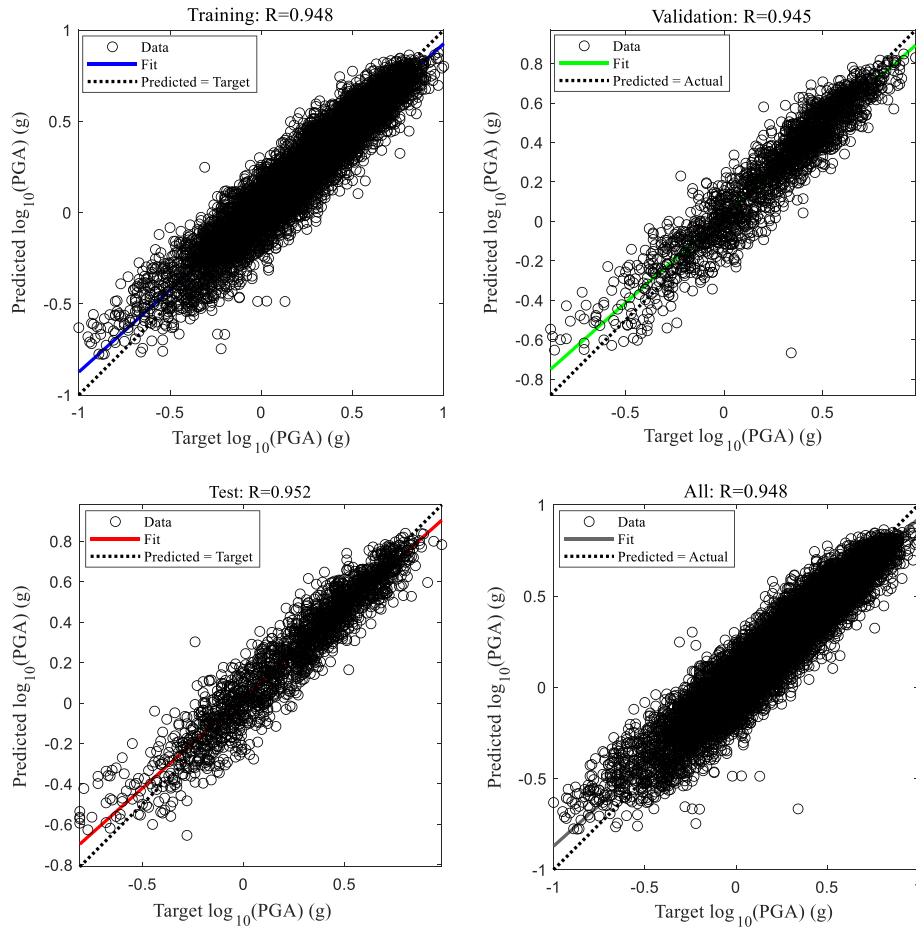


**FIGURE 6** Comparison of actual PGA with the predicted PGA from the developed ANN model.

**TABLE 2** Biases and weights of the ANN 4-7-1

Hidden node	Input-hidden weight				Hidden-output weight $\log_{10}(\text{PGA})$	Bias	
	$M_W$	$R_{hypo}$	$\log_{10}(R_{hypo})$	$\log_{10}(V_{s30})$		Hidden	Output
1	-1.5974	-0.9285	0.2424	-1.3628	-0.1262	1.7077	
2	0.1793	-0.0274	-2.3119	-0.6098	0.6633	2.1593	0.5310
3	5.7221	-1.9613	-0.7376	-0.3412	0.0830	-3.1907	
4	-2.7220	0.3865	0.5373	-0.0378	-0.3392	-1.2858	
5	0.6528	-1.1689	1.1899	0.3036	-0.6712	1.0580	
6	-0.9375	2.9341	-0.5128	0.9096	0.0911	0.2591	
7	-0.5685	1.9251	4.4336	0.8566	-0.0873	1.9032	

$$b = 0.1793 \times M_W - 0.0274 \times R_{hypo} - 2.3119 \times \log_{10}(R_{hypo}) - 0.6098 \times \log_{10}(V_{s30}) + 2.1593 \quad (7)$$

$$c = 5.7221 \times M_W - 1.9613 \times R_{hypo} - 0.7376 \times \log_{10}(R_{hypo}) - 0.3412 \times \log_{10}(V_{s30}) - 3.1907 \quad (8)$$

$$d = -2.7220 \times M_W + 0.3865 \times R_{hypo} + 0.5373 \times \log_{10}(R_{hypo}) - 0.0378 \times \log_{10}(V_{s30}) - 1.2858 \quad (9)$$

$$e = 0.6528 \times M_W - 1.1689 \times R_{hypo} + 1.1899 \times \log_{10}(R_{hypo}) + 0.3036 \times \log_{10}(V_{s30}) + 1.0580 \quad (10)$$

**TABLE 3** Limit of parameters used in this study

	Input parameters				Output parameter
	$M_W$	$R_{hypo}$	$\log_{10}(R_{hypo})$	$\log_{10}(V_{s30})$	$\log_{10}(PGA)$
Max	7.90	502.41	2.70	3.32	0.25
Min	3.20	2.06	0.31	1.95	-6.44

$$f = -0.9375 \times M_W + 2.9341 \times R_{hypo} - 0.5128 \times \log_{10}(R_{hypo}) + 0.9096 \times \log_{10}(V_{s30}) + 0.2591 \quad (11)$$

$$g = -0.5685 \times M_W + 1.9251 \times R_{hypo} + 4.4336 \times \log_{10}(R_{hypo}) + 0.8566 \times \log_{10}(V_{s30}) + 1.9032 \quad (12)$$

$$\begin{aligned} x = & -0.1262 \times \tanh(a) + 0.6633 \times \tanh(b) + 0.0830 \times \tanh(c) \\ & - 0.3392 \times \tanh(d) - 0.6712 \times \tanh(e) + 0.0911 \times \tanh(f) \\ & - 0.0873 \times \tanh(g) + 0.5310 \end{aligned} \quad (13)$$

$$\text{Normalized log - scaled PGA, } \log_{10}(PGA)_{normalized} = x \quad (14)$$

The normalised log-scaled ground motion parameter ( $\log_{10}(PGA)_{normalized}$ ) must be denormalized. Equation (15) yields the denormalized value of the log-scaled ground motion parameter ( $\log_{10}(PGA)$ ).

$$\begin{aligned} \log_{10}(PGA) = & 0.5(\log_{10}(PGA)_{normalized} + 1)(\log_{10}(PGA)_{max} \\ & - \log_{10}(PGA)_{min}) + \log_{10}(PGA)_{min} \end{aligned} \quad (15)$$

Only employ the log-scaled ground motion parameter prediction equation (Equation 15) in the dataset range where the ANN model was trained. The maximum and minimum input parameter limits are shown in Table 3.

Further, the effectiveness of the prediction equation should be assessed. This can be done by examining the residuals. The difference between the observed ground-motion value and the predicted value is referred to as residual in this study.

Figure 7 shows the distribution of residuals with respect to hypocentral distance, magnitude, and shear wave velocity. From the figure, it can be observed that the residuals show some random variability, but most of the average residuals are close to zero. The residual does not follow any trend with regard to the inputs as observed from this figure. Overall, the proposed model can predict ground motion values with high accuracy and is unaffected by any of the input variables.

## 6 | PARAMETRIC ANALYSIS

The effectiveness of the neural network model in capturing the physical phenomena exhibited by ground motion must now be evaluated. This can be achieved by performing the

parametric analysis with the predicted PGA values for various combinations of

$M_W$ ,  $R_{hypo}$ , and  $V_{s30}$ . Figure 8 shows the variation of PGA with respect to hypocentral distance for different magnitudes for  $V_{s30} = 760$  m/sec. The distance parameter in this study is the hypocentral distance. It stands for the distance between the source and the location. This measurement can provide a more accurate representation of the source-to-site distance since it is based on the earthquake's epicentre and focal depth. It can be observed that the PGA value increases with the earthquake's magnitude. The variation of the ground motion at different hypocentral distances with regard to magnitude can be seen in Figure 9, and it can be observed that the value of PGA decreases with respect to the distance parameter. From this figure, it can be affirmed that the predicted PGA increases with the magnitude and decreases with regard to the distance parameter.

The variation in ground motion values as a function of soil class is shown in Figure 10. Five types of soil are considered in this study based on shear wave velocity as per IBC [45]. The considered  $V_{s30}$  values are 1500 (A type), 1050 (B type), 525 (C type), 225 (D type), and 150 m/s (E type). The PGA value increases with the magnitude for all soil types. It can also be seen from the figure that the difference in the PGA value for a given magnitude is negligible for all soil types at a smaller distance ( $R_{hypo} = 10$  km). The opposite behaviour can be observed at a larger distance ( $R_{hypo} = 150$  km). When the soil type changes from soft (E type) to hard (A type), the PGA value decreases for all distances.

Overall, as demonstrated by the model's PGA patterns, the proposed model can capture the physical aspects of ground motion in terms of magnitude scaling, type of soil, and attenuation with respect to distance. As a result, for a given magnitude, hypocentral distance, and type of soil, the current model can generate reliable ground motion predictions.

## 7 | SENSITIVITY ANALYSIS

A sensitivity analysis was carried out to find the essential parameters and their relative relevance on the model outputs. The findings reveal that the network output varies depending on the inputs, providing insight into the most sensitive parameters that should be assessed more precisely. Here, the sensitivity analysis was done using the Cosine Amplitude Method [46]. According to this method, strength ratio between each input and output variable has been calculated using the Equation (16).

$$\text{Strength ratio} = \frac{\sum(\text{Input} \times \text{Output})}{\sqrt{\sum(\text{Input})^2 \times \sum(\text{Output})^2}} \quad (16)$$

On the dataset, Equation (16) is applied, and a graph is displayed as shown in Figure 11. As demonstrated in Figure 11, the Magnitude ( $M_w$ ) and Hypocentral distance ( $R_{hypo}$ ) are obviously the most effective components in the ground motion prediction model. The shear wave velocity ( $V_{s30}$ ) has the least influence on the prediction model when compared to magnitude and

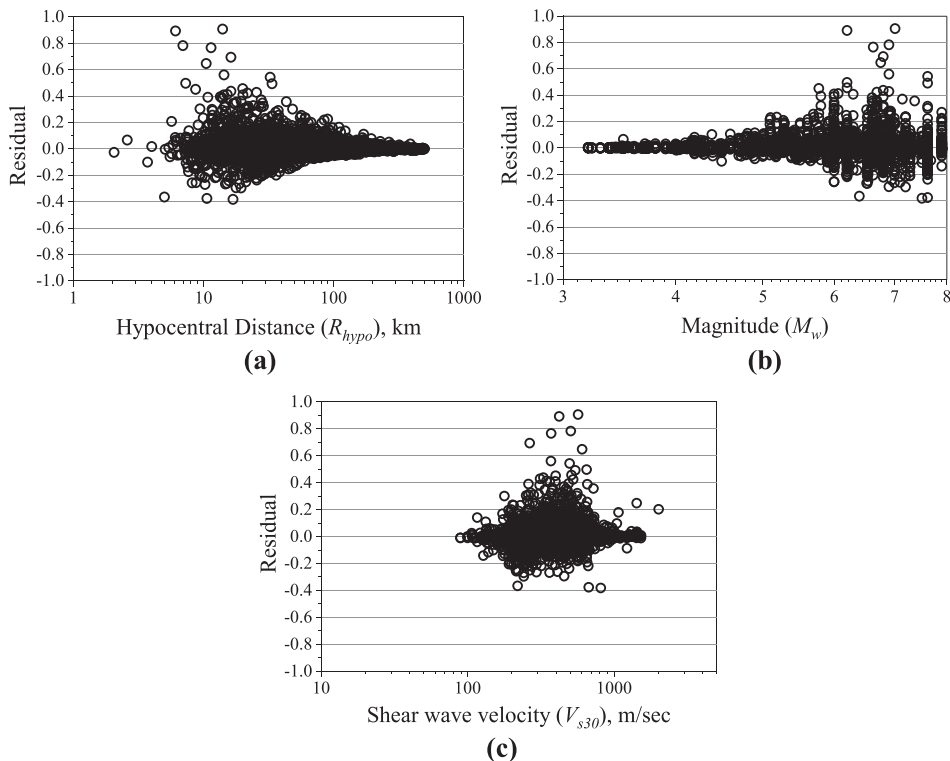


FIGURE 7 Distribution of residuals with respect to (a)  $R_{hypo}$ ; (b)  $M_w$ ; (c)  $V_{s30}$ .

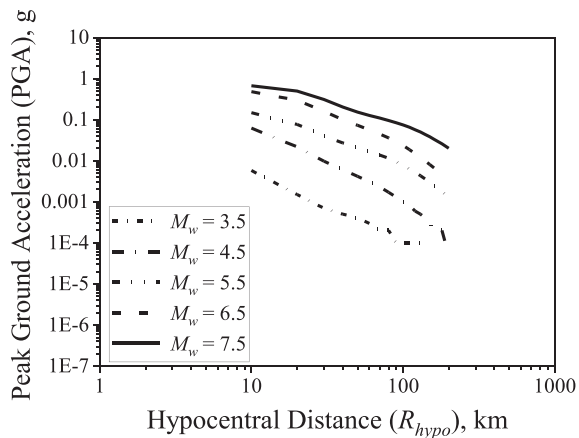


FIGURE 8 Variation of predicted PGA for different magnitudes with respect to hypocentral distance.

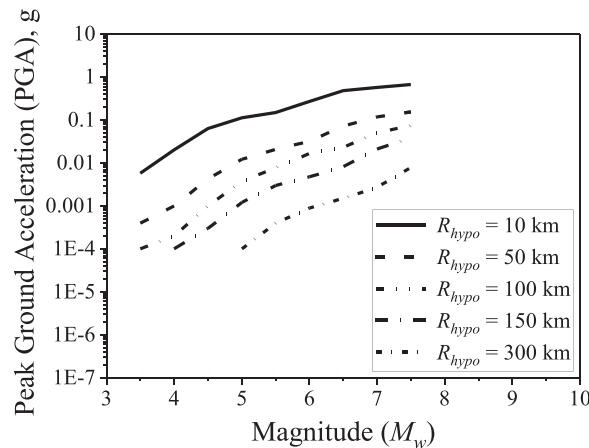


FIGURE 9 Variation of predicted PGA for different distances with respect to magnitude.

hypocentral distance. The order of relevance of input variables is as follows, according to the Cosine amplitude method:

Moment Magnitude ( $M_w$ ) > Hypocentral Distance ( $R_{hypo}$ ) > Shear Wave Velocity ( $V_{s30}$ )

### 8 | VALIDATION OF ANN PREDICTIVE RELATION

The new ground motion prediction equation may be used to estimate ground motion for future earthquakes. However, the new prediction equation must first be validated by compar-

ing with previous equations using global database. For such validation, the attenuation relationships developed by several researchers [47–49] were compared to the current equation. Figure 12 compares the variation of PGA produced by the past attenuation relations with the new ANN based prediction equation for different magnitudes. It is clear from the figure that the variation of PGA with the distance parameter from the developed ANN based equation is following the same trend as the known attenuation relationships. Because there are differences in input parameters evaluated, some deviations between equations are permissible. Also, an attempt has been made in

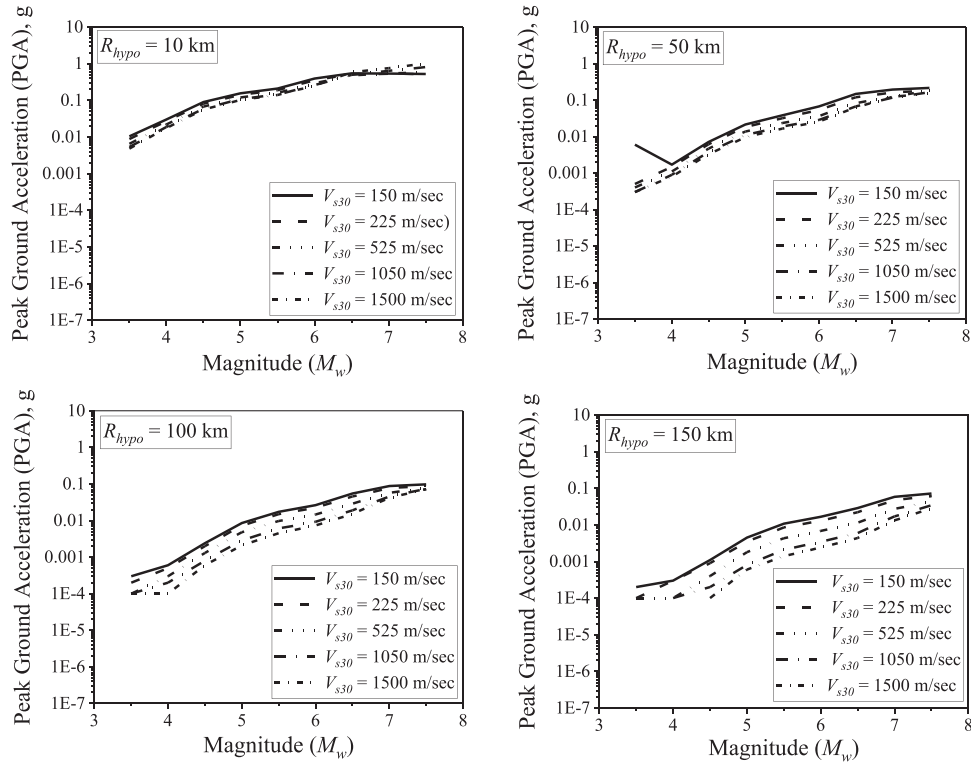


FIGURE 10 Variation of predicted PGA for different soil types with respect to magnitude.

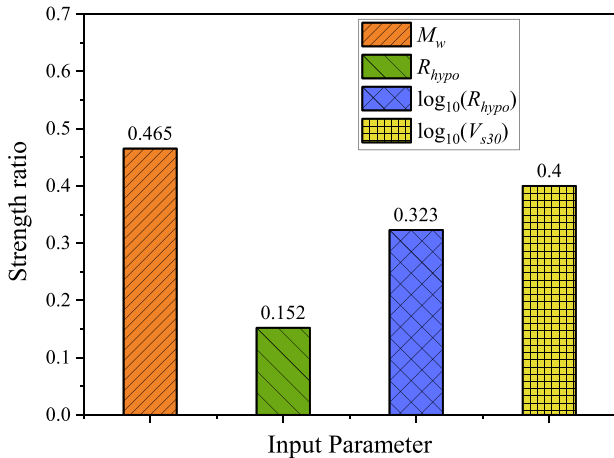


FIGURE 11 Strength ratios of different input variables.

this study to compare the predicted PGA values with those obtained from the existing model [50], which utilized the same updated NGA-West 2 database. The model in this work used the hypocentral distance, while the existing model considered the Joyner-Boore distance as a distance parameter. For a meaningful comparison, the hypocentral distance in the present study is converted to Joyner-Boore ( $R_{JB}$ ) distance using a magnitude-dependent conversion formula proposed in the study [51]. From Figure 13, it can be observed that the ANN model shows good agreement with the existing model. The slight variation in the PGA values is due to different input distance parameters.

In addition, the effectiveness of the new ANN-based equation in forecasting future events was tested in this study. In order to accomplish so, it should be able to determine the actual acceleration which was not included in the ANN model's training phase. Figure 14 depicts the actual and the predicted data of Chamoli earthquake (1999) recorded at different stations with soil type as rock. As per NEHRP guidelines, the shear wave velocity ( $V_{s30}$ ) is taken as 760 m/s. Recorded data from one more event with high magnitude was also used to validate the new prediction equation. Figure 15 shows the predicted PGAs of Hector Mine earthquake (1999) recorded at different stations (stiff soil). There is no evidence of a small hypocentral distance range in this earthquake's dataset. Figure 16 depicts the comparison between the actual recorded and predicted PGA values for San Fernando (1971) earthquake recorded at seven different stations with different soil profiles. The actual recorded data was taken from the PEER NGA database. It is clear that the newly constructed ANN-based prediction equation matches the actual recorded data quite well.

The residuals for the PGAs predicted using three different relationships are produced for quantitative analysis. Figure 17 shows the residual plots estimated using the proposed ANN model, existing models proposed by Boore DM et al. (2014) and Shiuly et al. (2020). The proposed ANN model predicts the ground motion value with lower residuals, as can be seen. This clearly demonstrates the proposed ANN model's ability to reliably predict PGA values with far smaller residuals than existing models.



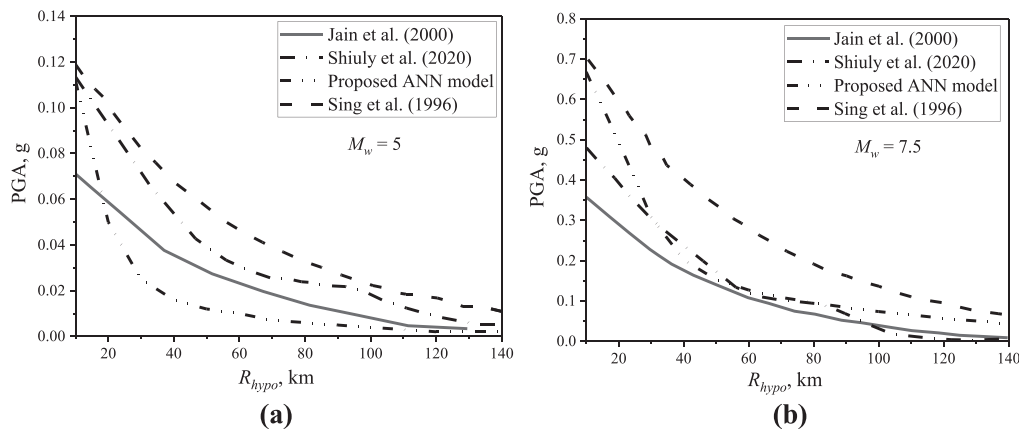


**FIGURE 12** Variation of PGA obtained by different existing relationships and developed ANN based relationship with  $V_{s30} = 760$  m/s for different magnitudes (a)  $M_w = 5$ ; (b)  $M_w = 7.5$ .

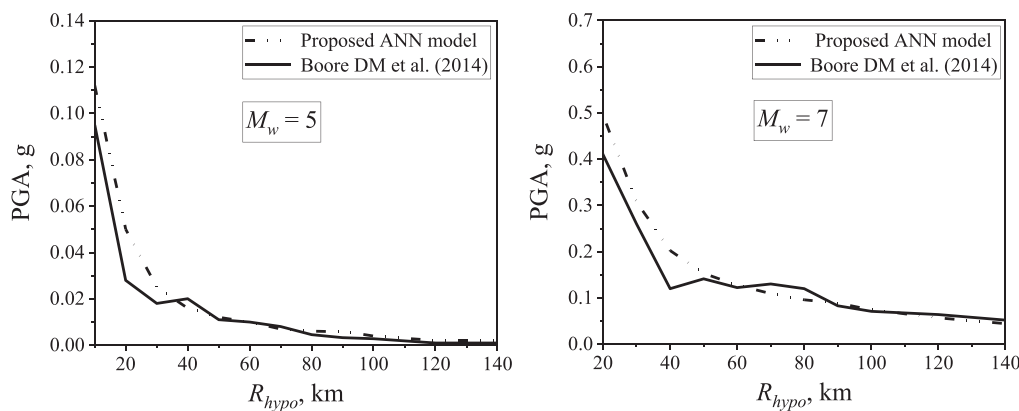


**FIGURE 13** Variation of PGA obtained by existing relationship and developed ANN model for NGA-West2 database for  $V_{s30} = 760$  m/s.

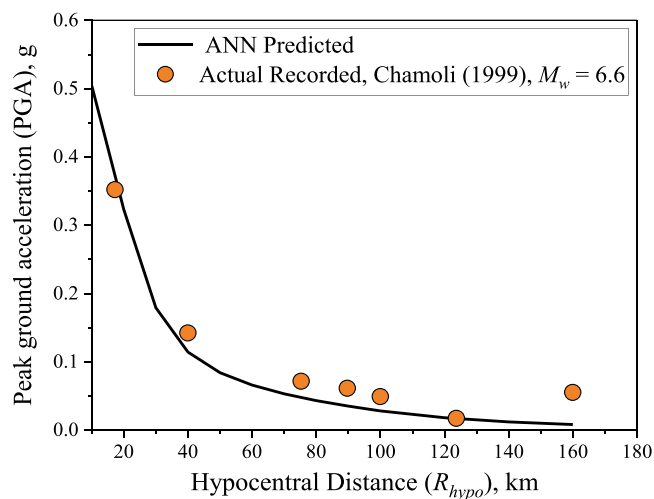


**FIGURE 14** Recorded data of Chamoli earthquake (1999), versus PGA, predicted using new equation.

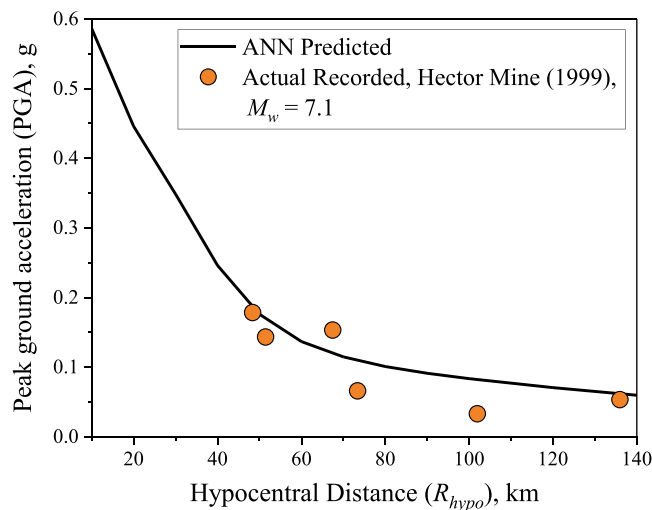


**FIGURE 15** Recorded data of Hector Mine earthquake (1999), versus PGA, predicted using new equation.

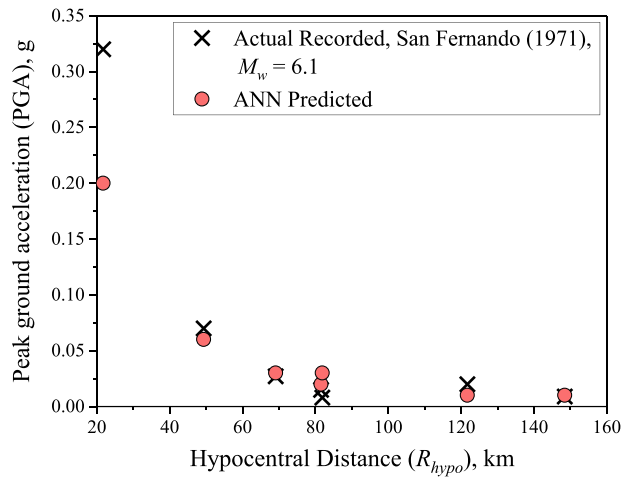


**FIGURE 16** Recorded data of San Fernando earthquake (1971), versus PGA, predicted using new equation.

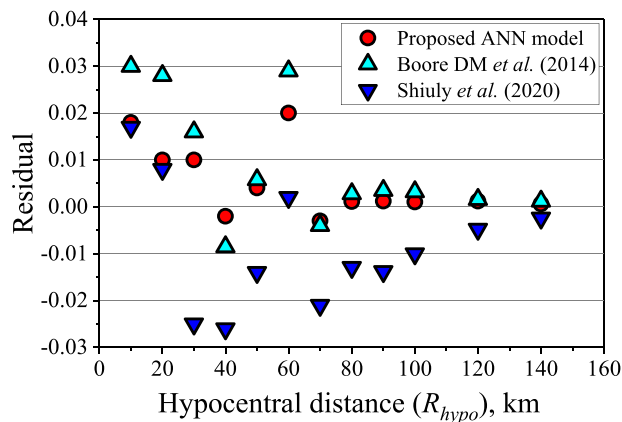


**FIGURE 17** Plot of residual between predicted and actual recorded PGAs.

## 9 | CONCLUSIONS

This goal of this work is to construct a prediction equation for ground motion parameter by utilizing the global database. The model is developed using 12,706 ground motion recordings from 283 earthquakes from the revised NGA-West2 database. Hypocentral distance ( $R_{hypo}$ ), shear wave velocity ( $V_{s30}$ ), and moment magnitude ( $M_w$ ), are considered as input parameters for the model. Peak Ground Acceleration (PGA) is considered as an output variable in the model development. The data in this study is modelled using a feed-forward neural network. The architecture of the ANN model (4-7-1) comprises of fully interconnected 4 input nodes, 7 hidden nodes and 1 output node. Using the trained weights and bias values, an ANN-based ground motion predictive equation was developed. In addition, the model was subjected to a sensitivity analysis.

The following are the conclusions drawn from this study:

1. The PGA from the prediction model increases with the magnitude and decreases with regard to the distance parameter.

2. The PGA value decreases as the soil type changes from soft (E type) to hard (A type).
3. In the dataset range for which the neural network was trained, the prediction equation can be employed, viz.  $3.2 \leq M_w \leq 7.9$ ,  $2.06 \leq R_{hypo} \leq 502.41$ , and  $89.32 \leq V_{s30} \leq 2100$ .
4. From the sensitivity study, it was concluded that moment magnitude and hypocentral distance are the most influential parameters on the performance of the model.
5. The proposed ANN model was validated and compared by determining its capacity to predict the recorded PGA of an event not included in the development of the model as precisely as feasible.
6. The residuals estimated using two existing models and the proposed model are compared. The residuals of the predicted values using the proposed ANN based model are significantly smaller.
7. The developed prediction equation may be utilized regardless of the location because the dataset used in this work includes a wide range of distances, magnitudes, and soil types.

This research demonstrates that an ANN-based technique for PGA prediction may be used as an alternate way for creating attenuation models by carefully leveraging the vast data base that has been collected throughout the world. The validity of the model, as well as their results and conclusions, are restricted to the database used in this study. In future research, the current ANN-based prediction equation can be further modified by including the fault mechanism, soil type, and focal depth as new input variables.

## AUTHOR CONTRIBUTIONS

S. P. Challagulla: Review and editing (equal). S. P. Challagulla: Conceptualization (lead); Methodology (lead); Data Curation (equal); writing—original draft (lead); formal analysis (lead); writing—review and editing (equal). E. Noroozinejad Farsangi: Software (lead); writing—review and editing (equal); Data Curation (equal). A. K. Suluguru: Data Curation (equal); writing—review and editing (equal). Mounika Manne: Data Curation (equal); writing—review and editing (equal).

## ACKNOWLEDGEMENTS

The authors would like to express their gratitude to the PEER group for their efforts in processing, merging, and making the various databases publicly available.

## CONFLICT OF INTEREST STATEMENT

The authors declare no conflicts of interest.

## DATA AVAILABILITY STATEMENT

The data that support the findings of this study are available from the corresponding author upon reasonable request.

## ORCID

Ehsan Noroozinejad Farsangi  <https://orcid.org/0000-0002-2790-526X>

## REFERENCES

1. Boore, D.M.: Stochastic simulation of high-frequency ground motions based on seismological models of the radiated spectra. *Bull. Seismol. Soc. Am.* 73(6A), 1865–1894 (1983)
2. Abrahamson, N.A., Silva, W.J.: Empirical response spectral attenuation relationships for shallow crustal earthquakes. *Seismol. Res. Lett.* 68(1), 94–127 (1997). <https://doi.org/10.1785/gssrl.68.1.94>.
3. McGuire, R.K.: Seismic ground motion parameter relations. *J. Geotech. Eng. Div.* 104(4), 481–490 (1978)
4. Boore, D.M., Joyner, W.B.: The empirical prediction of ground motion. *Bull. Seismol. Soc. Am.* 72(6B), S43–S60 (1982)
5. Peng, K., Wu, F.T., Song, L.: Attenuation characteristics of peak horizontal acceleration in northeast and southwest China. *Earthquake Eng. Struct. Dyn.* 13(3), 337–350 (1985)
6. Joyner, W.B., Boore, D.M.: Measurement, characterization, and prediction of strong ground motion. In: *Earthquake Engineering and Soil Dynamics II - Recent Advances in Ground-Motion Evaluation: Proceedings of the Specialty Conference*. New York, pp. 27–30 (1988)
7. Ambraseys, N.N., Bommer, J.J.: The attenuation of ground accelerations in Europe, pp. 675–678, *Earthquake Engineering, Tenth World Conference*, Balkema, Rotterdam (1991)
8. Atkinson, G.M., Boore, D.M.: Stochastic point-source modeling of ground motions in the Cascadia region. *Seismol. Res. Lett.* 68(1), 74–85 (1997)
9. Campbell, K.W., Bozorgnia, Y.: Updated near-source ground-motion (attenuation) relations for the horizontal and vertical components of peak ground acceleration and acceleration response spectra. *Bull. Seismol. Soc. Am.* 93(1), 314–331 (2003)
10. Atkinson, G.M.: Empirical attenuation of ground-motion spectral amplitudes in south-eastern Canada and the north-eastern United States. *Bull. Seismol. Soc. Am.* 94(3), 1079–1095 (2004)
11. Sharma, M.L., Douglas, J., Bungum, H., Kotadia, J.: Ground-motion prediction equations based on data from the Himalayan and Zagros regions. *J. Earthquake Eng.* 13(8), 1191–1210 (2009). <https://doi.org/10.1080/13632460902859151>.
12. Anbazhagan, P., Kumar, A., Sitharam, T.G.: Ground motion prediction equation considering combined dataset of recorded and simulated ground motions. *Soil Dyn. Earthquake Eng.* 53, 92–108 (2013). <https://doi.org/10.1016/j.soildyn.2013.06.003>.
13. Ramkrishnan, R., Sreevalsa, K., Sitharam, T.G.: Development of new ground motion prediction equation for the north and central himalayas using recorded strong motion data. *J. Earthquake Eng.* 25(0), 1903–1926 (2019). <https://doi.org/10.1080/13632469.2019.1605318>.
14. Ramkrishnan, R., Sreevalsa, K., Sitharam, T.G.: Strong motion data based regional ground motion prediction equations for North East India based on non-linear regression models. *J. Earthquake Eng.* 26(00), 2927–2947 (2020). <https://doi.org/10.1080/13632469.2020.1778586>.
15. Ashadi, A.L., Kaka, S.L.I.: Ground-motion relations for subduction-zone earthquakes in Java Island, Indonesia. *Arab. J. Sci. Eng.* 44(1), 449–465 (2019). <https://doi.org/10.1007/s13369-018-3563-x>.
16. Zhang, B., Yu, Y., Li, X., Wang, Y.: Ground motion prediction equation for the average horizontal component of PGA, PGV, and 5% damped acceleration response spectra at periods ranging from 0.033 to 8.0 s in southwest China. *Soil Dyn. Earthquake Eng.* 159, 107297 (2022)
17. Kumar, A., Ghosh, G., Gupta, P.K., Kumar, V., Paramasivam, P.: Seismic hazard analysis of Silchar city located in North East India. *Geomatics, Nat. Hazards Risk* 14(1), 2170831 (2023)
18. Chen, W., Wang, D., Zhang, C., Yao, Q., Si, H.: Estimating seismic intensity maps of the 2021 M w 7.3 Madoi, Qinghai and M w 6.1 Yangbi, Yunnan, China earthquakes. *J. Earth Sci.* 33(4), 839–846 (2022)
19. Khosravikia, F., Clayton, P.: Machine learning in ground motion prediction. *Comput. Geosci.* 148(January), 104700 (2021). <https://doi.org/10.1016/j.cageo.2021.104700>.
20. Kerh, T., Ting, S.B.: Neural network estimation of ground peak acceleration at stations along Taiwan high-speed rail system. *Eng. Appl. Artif. Intell.* 18(7), 857–866 (2005)
21. Ahmad, I., El Naggar, M.H., Khan, A.N.: Neural network based attenuation of strong motion peaks in Europe. *J. Earthq. Eng.* 12(5), 663–680 (2008)
22. Asencio-Cortés, G., Martínez-Álvarez, F., Troncoso, A., Morales-Esteban, A.: Medium-large earthquake magnitude prediction in Tokyo with artificial neural networks. *Neural Comput. Appl.* 28(5), 1043–1055 (2017)
23. Günaydın, K., Günaydın, A.: Peak ground acceleration prediction by artificial neural networks for north-western Turkey. *Math. Probl. Eng.* 2008, 1–20 (2008)
24. Wiszniowski, J.: Estimation of a ground motion model for induced events by Fahlman's cascade correlation neural network. *Comput. Geosci.* 131, 23–31 (2019)
25. Pathak, J., Paul, D.K., Godbole, P.N.: ANN based attenuation relationship for estimation of PGA using Indian strong-motion data. In *Proceedings of First European Conference on Earthquake Engineering and Seismology* (a joint event of the 13th ECEE & 30th General Assembly of the ESC) (2006)
26. Dhanya, J., Raghukanth, S.T.G.: Neural network-based hybrid ground motion prediction equations for Western Himalayas and North-Eastern India. *Acta Geophys.* 68(2), 303–324 (2020)
27. Klimasewski, A., Sahakian, V., Thomas, A.: Comparing artificial neural networks with traditional ground-motion models for small-magnitude earthquakes in Southern California. *Bull. Seismol. Soc. Am.* 111(3), 1577–1589 (2021)
28. Açığenç, M., Ulaş, M., Alyamaç, K.E.: Using an artificial neural network to predict mix compositions of steel fiber-reinforced concrete. *Arab. J. Sci. Eng.* 40(2), 407–419 (2015). <https://doi.org/10.1007/s13369-014-1549-x>.
29. Sharma, N., Dasgupta, K., Dey, A.: Prediction of natural period of RC frame with shear wall supported on soil-pile foundation system using artificial neural network. *J. Earthquake Eng.* 26(00), 4147–4171 (2020). <https://doi.org/10.1080/13632469.2020.1824876>.
30. Oh, B.K., Park, Y., Park, H.S.: Seismic response prediction method for building structures using convolutional neural network. *Struct. Control Heal. Monit.* 27(5), 1–17 (2020). <https://doi.org/10.1002/stc.2519>.
31. Zhang, B., Wang, K., Lu, G., Guo, W.: Seismic response analysis and evaluation of laminated rubber bearing supported bridge based on the artificial neural network. *Shock Vib.* 2021, 5566874 (2021). <https://doi.org/10.1155/2021/5566874>.
32. Liu, T., Dai, Z.: Real-time prediction of the trend of ground motion intensity based on deep learning. *Shock Vib.* 2021, 5518204 (2021). <https://doi.org/10.1155/2021/5518204>.
33. Khosravikia, F., Clayton, P., Nagy, Z.: Artificial neural network-based framework for developing ground-motion models for natural and induced earthquakes in Oklahoma, Kansas, and Texas. *Seismol. Res. Lett.* 90(2A), 604–613 (2019)
34. Novakovic, M., Atkinson, G.M., Assatourians, K.: Empirically calibrated ground-motion prediction equation for Oklahoma. *Bull. Seismol. Soc. Am.* 108(5A), 2444–2461 (2018)
35. Challagulla, S.P., Parimi, C., Anmala, J.: Prediction of spectral acceleration of a light structure with a flexible secondary system using artificial neural networks. *Int. J. Struct. Eng.* 10(4), 353–379 (2020)
36. Challagulla, S.P., Parimi, C., Pradeep, S., Farsangi, E.: Estimation of dynamic design parameters for buildings with multiple sliding non-structural elements using machine learning. *Int. J. Struct. Eng.* 11, 147–172 (2021). <https://doi.org/10.1504/IJSTRUCTE.2021.10034438>.
37. Challagulla, S.P., Bhargav, N.C., Parimi, C.: Evaluation of damping modification factors for floor response spectra via machine learning model. *Structures* 39, 679–690 (2022)
38. Raza, A., et al.: Prediction of axial load-carrying capacity of GFRP-reinforced concrete columns through artificial neural networks. *Structures* 28, 1557–1571 (2020)
39. Hakim, G.P.N., et al.: Levenberg Marquardt artificial neural network model for self-organising networks implementation in wireless sensor network. *IET Wirel. Sens. Syst.* (2023). <https://doi.org/10.1049/wss2.12052>
40. Shahin, M.A., Jaksa, M.B., Maier, H.R.: Artificial neural network based settlement prediction formula for shallow foundations on granular soils. *Aust. Geomech. J. News Aust. Geomech. Soc.* 37(4), 45 (2002)
41. Hecht-Nielsen, R.: Theory of the backpropagation neural network. In: *Neural Networks for Perception*, pp. 65–93. Elsevier, Amsterdam (1992)

42. Dhanya, J., Raghukanth, S.T.G.: Ground motion prediction model using artificial neural network. *Pure Appl. Geophys.* 175(3), 1035–1064 (2018). <https://doi.org/10.1007/s00024-017-1751-3>.
43. Debnath, S., Sultana, P.: Prediction of settlement of shallow foundation on cohesionless soil using artificial neural network. In *Proceedings of the 7th Indian Young Geotechnical Engineers Conference: 7IYGEC-2019* (pp. 477–486). Singapore: Springer Singapore (2019)
44. Goh, A.T.C., Kulhawy, F.H., Chua, C.G.: Bayesian neural network analysis of undrained side resistance of drilled shafts. *J. Geotech. Geoenviron. Eng.* 131(1), 84–93 (2005)
45. Council, I.C.: International Building Code 2018. *Intl Code Councl. Washington, DC, USA* (2018)
46. Monjezi, M., Hasanipanah, M., Khandelwal, M.: Evaluation and prediction of blast-induced ground vibration at Shur River Dam, Iran, by artificial neural network. *Neural Comput. Appl.* 22(7), 1637–1643 (2013)
47. Jain, S.K., Roshan, A.D., Arlekar, J.N., Basu, P.C.: Empirical attenuation relationships for the Himalayan earthquakes based on Indian strong motion data. In: *Proceedings of the Sixth International Conference on Seismic Zonation*. Palm Springs, CA, pp. 12–15 (2000)
48. Singh, R.P., Aman, A., Prasad, Y.J.J.: Attenuation relations for strong seismic ground motion in the Himalayan region. *Pure Appl. Geophys.* 147(1), 161–180 (1996)
49. Shiuly, A., Roy, N., Sahu, R.B.: Prediction of peak ground acceleration for Himalayan region using artificial neural network and genetic algorithm. *Arab. J. Geosci.* 13(5), 215 (2020). <https://doi.org/10.1007/s12517-020-5211-5>.
50. Boore, D.M., Stewart, J.P., Seyhan, E., Atkinson, G.M.: NGA-West2 equations for predicting PGA, PGV, and 5% damped PSA for shallow crustal earthquakes. *Earthquake Spectra* 30(3), 1057–1085 (2014). <https://doi.org/10.1193/070113EQS184M>.
51. Laouami, N., Slimani, A., Larbes, S.: Ground motion prediction equations for Algeria and surrounding region using site classification based H/V spectral ratio. *Bull. Earthquake Eng.* 16(7), 2653–2684 (2018). <https://doi.org/10.1007/s10518-018-0310-3>.

**How to cite this article:** Challagulla, S.P., Suluguru, A.K., Farsangi, E.N., Manne, M.: Application of metaheuristic algorithms in prediction of earthquake peak ground acceleration. *J. Eng.* 2023, 1–12 (2023). <https://doi.org/10.1049/tje2.12269>